J. Plasma Physics (2011), *vol.* 77, *part* 3, *pp.* 419–429. © Cambridge University Press 2010
doi:10.1017/S0022377810000632

Space-charge waves in a relativistic electron beam with ion-channel guiding

SAEED MIRZANEJHAD[1], BEHROUZ MARAGHECHI[2], FARSHAD SOHBATZADEH[1] and IMAN KAMEL-JAHROMI[1]

[1]Department of Physics, Faculty of Basic Science, University of Mazandaran, P.O. Box 47416-95447, Babolsar, Iran
(saeed@umz.ac.ir)

[2]Department of Physics, Amirkabir University of Technology, P.O. Box 15875-4413, Tehran, Iran

(Received 11 May 2010, revised 10 September 2010 and accepted 11 September 2010, first published online 5 November 2010)

Abstract. Space-charge waves in a relativistic electron beam that completely fills a cylindrical metallic waveguide and is guided by an ion channel are analyzed numerically. Equilibrium consists of a uniform and rigid rotation without betatron oscillations. Using cold fluid equations a differential equation and boundary conditions are derived that constitute an eigenvalue problem. This eigenvalue problem is solved, numerically, with the finite difference scheme using shooting method. Dispersion characteristics and electrostatic potential structures of azimuthally symmetric and nonsymmetric space-charge waves are studied. Perfect agreement with analytical results at asymptotic limit of zero axial velocity is found. It was found that relativistic effects modify the dispersion characteristics of the space-charge waves considerably and can concentrate the electric field energy of the wave into a thin and small shell around the axis.

1. Introduction

Space-charge waves resulting from the longitudinal bunching of charged particles occur in the nonneutral plasmas including charged particle beams. Their application range from waves observed in space plasmas [1, 2], and laboratory including charged particle accelerators, heavy ion fusion [3], and free electron lasers [4, 5].

In nonneutral plasmas, Diocotron modes are investigated in [6–11] and electrostatic modes are studied analytically in [12–16] and numerically in [17] and [18]. Space-charge waves in electron beams are investigated experimentally [19–23] as well as theoretically [24–30]. Recently, in the X-ray free-electron laser, longitudinal space charge [24, 31] has been found to be responsible for the microbunching instability [32–34], where the high-frequency components of the beam current produce energy modulations at the same frequencies due to longitudinal space charge.

The purpose of the present study is the numerical investigation of the dispersion characteristic and the electric-field structure of space-charge waves in a relativistic electron beam with ion-channel guiding inside a cylindrical and metallic waveguide. Recently, ion-channel guiding has been proposed as an alternative focusing method to replace axial magnetic field for guiding charged particle beams. In this method, a

https://doi.org/10.1017/S0022377810000632 Published online by Cambridge University Press

relativistic electron beam, in passing through a preionized plasma, ejects the electrons and will be guided by the positive ion core. This alternative technique was first used for the transport of the relativistic electron beam by Martin et al. [35] and was applied in the advanced test accelerator by Caporaso et al. [36] Ion-channel guiding was first proposed by Takayama and Hiramatsu [37] for use in free-electron laser and was experimentally demonstrated by Ozaki et al. [38] and Yu et al. [39].

Characteristics of waves in a relativistic electron beam with ion-channel guiding depend very much on the equilibrium configuration of the beam. Eigenmodes of a nonrotating electron beam under ion-focused regime in which electrons make small amplitude betatron oscillations, in the combined fields of the ion-channel and self-fields of the beam, have been analyzed by Rouhani and Maraghechi [40]. Because electrons can only obtain a small transverse oscillatory energy due to the ion charge field, the gain of such a system is very low. On that basis, possibility of employing the cyclotron electron beam in the ion channel is proposed in [41]. This new plasma maser scheme is called ion-channel electron cyclotron maser.

In the present investigation of space-charge waves, equilibrium consists of a rigid rotation of the electron beam without any betatron oscillation. Contrary to [40], no analytical solutions are possible to find and a numerical method is used to find the frequency and the electrostatic potential of space-charge waves. The eigenvalue problem will be solved by the finite difference scheme using shooting method. In the asymptotic limit of zero axial velocity, numerical results are checked with the analytical results with a very good agreement. It was shown that dispersion characteristics and electric field structures of space-charge waves of a relativistic electron beam are considerably different than that of a nonrelativistic beam with ion-channel guiding. Relativistic effects push the electric field energy toward the axis and concentrate it into a thin cylindrical shell, which becomes thinner and moves toward the axis as the energy of the beam is increased. This can have important applications in free-electron devices for the generation of electromagnetic radiation that relies on the space-charge waves.

The wave–wave interaction in the electrostatic perturbation of a rotating non-neutral plasma with an axial magnetic field has been studied by Stenflo [42], and the possibility of instability has been reported. The present problem is similar to [42] except for the axial magnetic field, which is replaced by the electric field of an ion channel and the lack of analytical solution in the linear analysis of our case. Although this might be an interesting problem, these differences may make the analysis of wave–wave interaction in the present problem rather difficult.

Organization of the paper is as follows. In Sec. 2, a differential equation for the electrostatic potential is found using the cold fluid model. In Sec. 3, the finite difference method is used to solve the eigenvalue problem for the azimuthally symmetric and nonsymmetric modes. In Sec. 4, concluding remarks are made.

2. The eigenvalue problem

A relativistic and cold electron beam, with the lab-frame density n_b and axial velocity $\beta_0 = v_0/c$, passes through, and completely fills, a cylindrical and metallic waveguide with radius r_b. Focusing of the electron beam against the self-fields of the beam is provided by an ion channel, with the lab-frame density n_i, that also fills the waveguide. Equilibrium fields are due to the ion-channel and the self-electric (due to

https://doi.org/10.1017/S0022377810000632 Published online by Cambridge University Press

the electronic charge) and self-magnetic (due to the axial motion) fields of electrons. Equilibrium velocity consists of a uniform and relativistic axial motion plus a rigid rotation with a constant frequency to provide the confinement.

To find the frequency of the rigid rotation of the beam, the force balance equation, in the lab frame, can be written as follows:

$$-\gamma n r\omega_r^2 = -2\pi n_b e^2 r\left\{\left(\frac{n_i}{n_b}\right) - \frac{r_b^2\omega_r^2}{c^2}\left(1-\frac{r^2}{r_b^2}\right) + \beta_0^2\right\}, \tag{1}$$

where $\gamma = (1-\beta_0^2)^{-1/2}$ is the relativistic factor. The first term, at the right-hand side of (1), is due to the electric field of the ion-channel and the self-electric field of electrons, and the second and third terms are due to the axial and azimuthal self-magnetic fields, respectively, produced by the azimuthal and axial velocities. Assuming nonrelativistic azimuthal rotations, i.e. $(r_b^2\omega_r^2)/c^2 \ll 1$, the second term can be neglected to obtain the rotation frequency of the beam

$$\omega_r = \omega_i\left(1-\frac{n_b}{\gamma^2 n_i}\right)^{1/2}, \tag{2}$$

where $\omega_i = (2\pi n_i e^2/\gamma m)^{1/2}$ is the betatron frequency.

The equilibrium, in the beam frame, is described in cylindrical coordinates (r,θ,z) by the following velocity and fields:

$$\vec{V}_0 = \gamma r\omega_r\hat{\theta}, \tag{3}$$

$$\vec{E}_0 = 2\pi e\gamma n_i\left(1-\frac{n_b}{\gamma^2 n_i}\right)\vec{r}, \tag{4}$$

$$\vec{B}_0 = -2\pi e\gamma n_i\beta_0 r\hat{\theta}. \tag{5}$$

Equation (5) is the magnetic field of ions as appears to the stationary electrons.

Perturbed state consists of a space-charge wave with electrostatic perturbations $\tilde{\varphi}$, $\tilde{\vec{V}}$, and $\tilde{n}$, propagating in the z direction, with the space and time dependency $\tilde{\psi}(r)e^{i(kz+l\theta-\omega t)}$. Since the electrostatic approximation is assumed in the beam frame, the electromagnetic effects of the space-charge wave, in the lab frame, is included in the analysis. In the beam frame, small amplitude oscillation can be described by a nonrelativistic cold fluid model with the following linearized equations:

$$\frac{\partial\tilde{n}}{\partial t} + \frac{n_b}{\gamma}\nabla.\tilde{\vec{V}} + \vec{V}_0.\nabla\tilde{n} = 0, \tag{6}$$

$$\frac{\partial\tilde{\vec{V}}}{\partial t} + (\vec{V}_0.\nabla)\tilde{\vec{V}} + (\tilde{\vec{V}}.\nabla)\vec{V}_0 = \frac{e}{m}\nabla\tilde{\varphi} - \frac{e}{m}\frac{\tilde{\vec{V}}\times\vec{B}_0}{c}, \tag{7}$$

$$\nabla^2\tilde{\varphi} = 4\pi e\tilde{n}. \tag{8}$$

The momentum (7) can be used to find the velocity component in terms of the electrostatic potential $\tilde{\varphi}$ as

$$\tilde{V}_r = i\frac{e}{m\eta}\frac{\chi_1}{\chi_0}\tilde{\varphi}, \tag{9}$$

$$\tilde{V}_\theta = -\frac{e}{m\eta}\frac{\chi_2}{\chi_0}\tilde{\varphi}, \tag{10}$$

https://doi.org/10.1017/S0022377810000632 Published online by Cambridge University Press

$$\tilde{V}_z = -\frac{e}{m\eta}\frac{\chi_3}{\chi_0}\tilde{\varphi}, \tag{11}$$

with

$$\chi_0 = \eta^2 - 4\gamma^2\omega_r^2 - \omega_i^4\gamma^4\beta_0^2\frac{r^2}{c^2}, \tag{12}$$

$$\chi_1 = -2\gamma\omega_r\eta\frac{l}{r} + \omega_i^2\gamma^2\beta_0\eta k\frac{r}{c} + \eta^2\frac{\partial}{\partial r}, \tag{13}$$

$$\chi_2 = \eta^2\frac{l}{r} - \omega_i^2\gamma^2\beta_0\left(\omega_i^2\gamma^2\beta_0\frac{l}{c} + 2\gamma\omega_r k\right)\frac{r}{c} - 2\gamma\omega_r\eta\frac{\partial}{\partial r}, \tag{14}$$

$$\chi_3 = k\eta^2 - 2\gamma\omega_r\left(2\gamma\omega_r k + \omega_i^2\gamma^2\beta_0\frac{l}{c}\right) + \omega_i^2\gamma^2\beta_0\eta\frac{r}{c}\frac{\partial}{\partial r}, \tag{15}$$

$$\eta = \omega - l\gamma\omega_r. \tag{16}$$

Equations (9)–(11) may be substituted in the continuity (6) to obtain

$$\tilde{n} = \frac{en_b}{m\gamma\eta^2}\left[\frac{1}{r}\frac{\partial}{\partial r}\left(r\frac{\chi_1}{\chi_0}\right) - \frac{l}{r}\frac{\chi_2}{\chi_0} - k\frac{\chi_3}{\chi_0}\right]\tilde{\varphi}. \tag{17}$$

The density $\tilde{n}$, from (17), will be substituted in the Poison equation (8) to obtain the differential equation for the electrostatic potential $\tilde{\varphi}$ as

$$\left[\frac{1}{r}\frac{\partial}{\partial r}\left(r\frac{\partial}{\partial r}\right) - \frac{\omega_p^2}{\eta^2}\frac{1}{r}\frac{\partial}{\partial r}\left(r\frac{\chi_1}{\chi_0}\right) - \frac{l^2}{r^2} - k^2 + \frac{\omega_p^2}{\eta^2}\left(\frac{l}{r}\frac{\chi_2}{\chi_0} + k\frac{\chi_3}{\chi_0}\right)\right]\tilde{\varphi} = 0, \tag{18}$$

where $\omega_p = (4\pi n_b e^2/\gamma m)^{1/2}$ is the relativistic plasma frequency in the lab frame. The boundary conditions are the regularity of solution at the center and vanishing of the potential on the metallic boundary, i.e.

$$\tilde{\varphi}_{(r=0)} = \text{finite} \quad \text{and} \quad \tilde{\varphi}_{(\mathrm{r=r_b})} = 0. \tag{19}$$

Equation (18), along with the boundary conditions (19), constitutes an eigenvalue problem for ω. This equation will be solved by the finite difference scheme using shooting method.

For the zero axial velocity $v_0 = 0$, (18) will reduce to the Bessel differential equation,

$$\frac{1}{r}\frac{\partial}{\partial r}\left[r\frac{\partial}{\partial r}\tilde{\varphi}\right] - \frac{l^2}{r^2}\tilde{\varphi} - T^2\tilde{\varphi} = 0 \tag{20}$$

with

$$T^2 = \mathrm{k}^2\frac{\left(1 - \dfrac{\omega_p^2}{(\omega - l\omega_r)^2}\right)}{\left(1 - \dfrac{\omega_p^2}{(\omega - l\omega_r)^2 - 4\omega_r^2}\right)}. \tag{21}$$

Equation (20) with the boundary conditions (19) has an analytical solution

$$\tilde{\varphi} \sim J_l(Tr) \tag{22}$$

with the dispersion relation

$$T = P_{lm}, \quad m = 1, 2, \ldots \tag{23}$$

https://doi.org/10.1017/S0022377810000632 Published online by Cambridge University Press

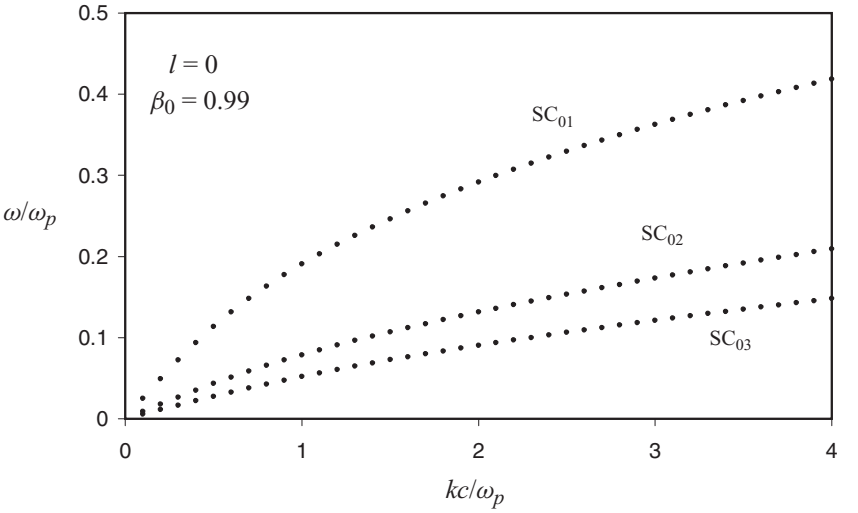


Figure 1. Dispersion curves for symmetric ($l = 0$) space-charge modes with $n_i = 10^{13}\,\mathrm{cm}^{-3}, n_b = 10^{12}\,\mathrm{cm}^{-3}$, and $\beta_0 = 0.99$.

where P_{lm} is mth zero of $J_l(x)$ (the Bessel function of the first kind and of order l). Therefore, space-charge modes are abbreviated as SC_{lm}.

3. Numerical procedure and results

The eigenvalue problem (18) and (19) does not have an analytical solution and must be solved numerically. This problem is solved, in this section, by the finite difference scheme using a shooting method to find the eigenvalue ω and the eigenfunction $\tilde{\varphi}$. Therefore, dispersion characteristics and the field structures of space-charge waves can be studied.

We will solve (18) by the finite difference scheme from the origin ($r = 0$) with an arbitrary value for the electrostatic potential ($\tilde{\varphi}(r = 0) =$ finite). Equation (18) is a second-order ordinary differential equation, and its solution has two constants of integration. To evaluate these constants, two values for $\tilde{\varphi}$ at two different points are required. These two points are preferably on the axis $r = 0$ and on the waveguide boundary at $r = r_b$ provided that they also specify the amplitude of the wave, otherwise, the amplitude also needs to be given.

The left-hand side of the Poisson equation (18) contains terms proportional to $1/r$ and $1/r^2$; therefore, $\tilde{\varphi}$ or $\mathrm{d}\tilde{\varphi}/\mathrm{d}r$ need to have some specific values to prevent $\nabla^2\tilde{\varphi}$ from becoming infinite at $r = 0$. To obtain the correct boundary condition on the waveguide wall, i.e. $\tilde{\varphi}(r = r_b) = 0$, the wave frequency ω is used as the adjustment parameter in the shooting method. The electrostatic potential slope at the origin is $(\mathrm{d}\tilde{\varphi}/\mathrm{d}r)\,|_{r=0} = 0$ for the $l = 0$ case and an arbitrary $(\mathrm{d}\tilde{\varphi}/\mathrm{d}r)\,|_{r=0}$ for the $l = 1$ case, in accordance with (24).

Dispersion curves and electrostatic potential structures of space-charge waves are studied. In the numerical method, solutions are not Bessel functions but still the same notation SC_{lm} is used for the space-charge modes, where m is the number of radial nodes, i.e. number of zeros of $\tilde{\varphi}$ between $r = 0$ and $r = r_b$. Figures 1 and 2

https://doi.org/10.1017/S0022377810000632 Published online by Cambridge University Press

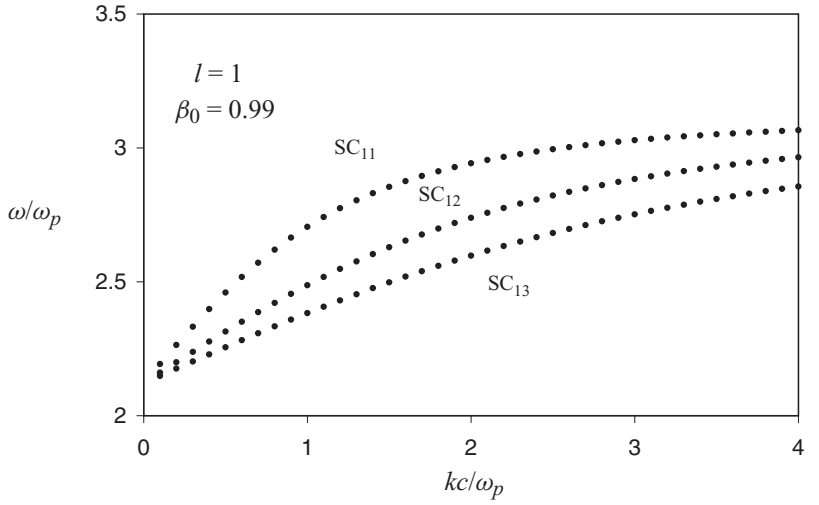


Figure 2. Dispersion curves for nonsymmetric ($l = 1$) space-charge modes with $n_i = 10^{13}\,\mathrm{cm}^{-3}, n_b = 10^{12}\,\mathrm{cm}^{-3}$, and $\beta_0 = 0.99$.

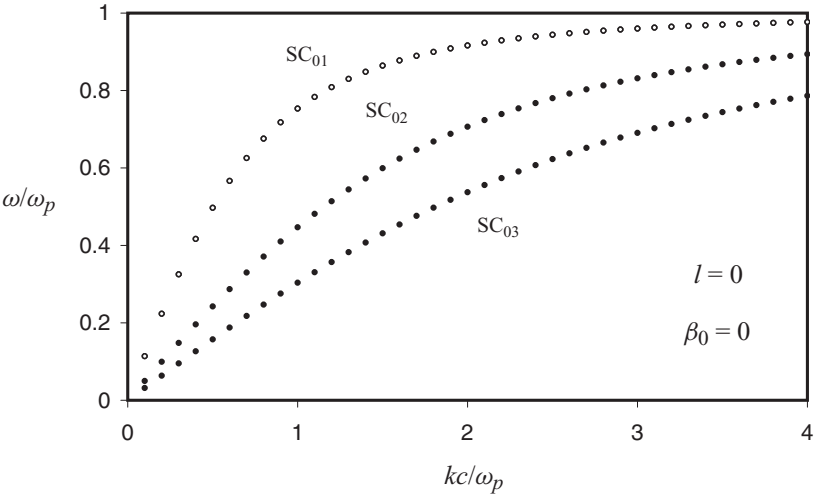


Figure 3. Dispersion curves for symmetric ($l = 0$) space-charge modes with zero axial velocity and with $n_i = 10^{13}\,\mathrm{cm}^{-3}$, and $n_b = 10^{12}\,\mathrm{cm}^{-3}$. Hollow circles are from analytical solutions.

show the dispersion curves for the symmetric ($l = 0$) and nonsymmetric ($l = 1$) modes with $n_i = 10^{13}\,\mathrm{cm}^{-3}$, $n_b = 10^{12}\,\mathrm{cm}^{-3}$, and $\beta_0 = 0.99$. Symmetric modes start from zero frequency at $k = 0$ and approach their asymptotic values for frequency gradually, while nonsymmetric modes start from nonzero frequency and approach their asymptotic frequency at relatively smaller value of k. Nonsymmetric modes have higher frequency compared to the corresponding symmetric mode. Dispersion curves for symmetric ($l = 0$) modes and for the zero axial velocity $\beta_0 = 0$ are shown in Fig. 3. Hollow circles are obtained from the analytic solution of (23) for SC_{01} mode and are almost on the points that are obtained from the numerical solution

https://doi.org/10.1017/S0022377810000632 Published online by Cambridge University Press

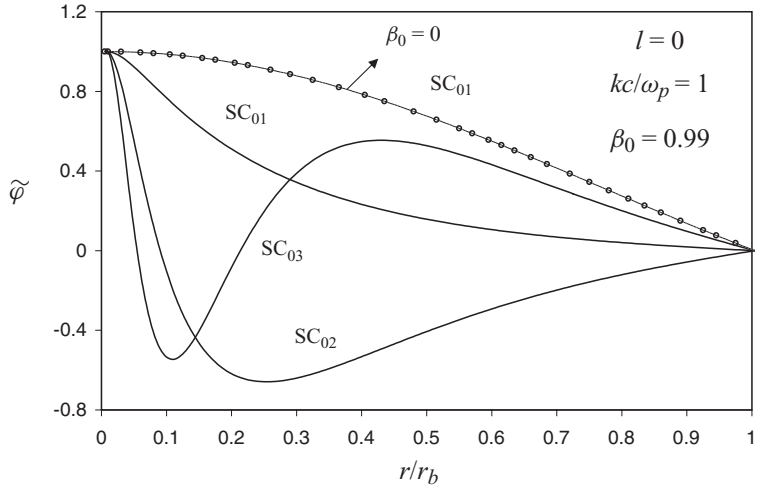


Figure 4. Electrostatic potential $\tilde{\varphi}$ as a function of the normalized radial distance r/r_b for symmetric ($l = 0$) modes, for $n_i = 10^{13}\,\mathrm{cm}^{-3}$, $n_b = 10^{12}\,\mathrm{cm}^{-3}$, $kc/\omega_p = 1$, and $\beta_0 = 0.99$. The curve from the numerical solution coincides with hollow circles that are from the analytical solutions of SC_{01} mode with $\beta_0 = 0$.

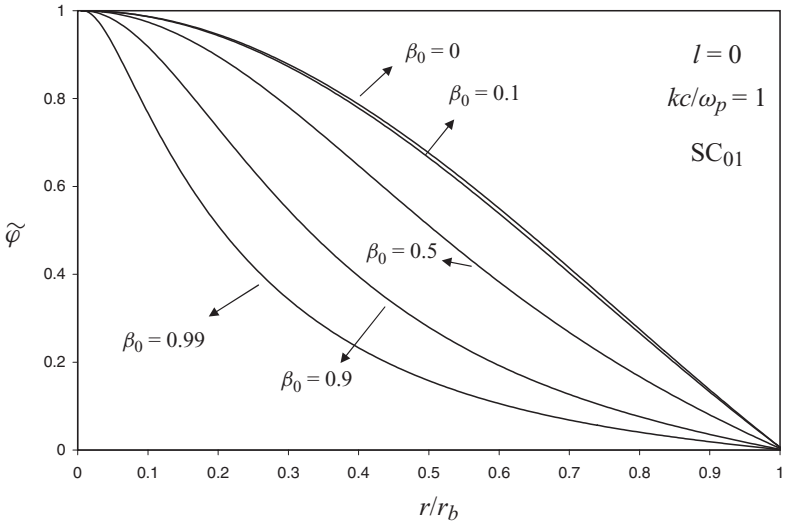


Figure 5. Electrostatic potential $\tilde{\varphi}$ of SC_{01} mode as a function of the normalized radial distance r/r_b for different beam velocity β_0, $n_i = 10^{13}\,\mathrm{cm}^{-3}$, $n_b = 10^{12}\,\mathrm{cm}^{-3}$, and $kc/\omega_p = 1$.

of the eigenvalue problem. This almost shows a perfect agreement between the numerical and analytical results.

Electrostatic potential structures of space-charge waves are also investigated. Electrostatic potential $\tilde{\varphi}$ profile of the transverse plane is shown in Figs. 4 and 5 for the symmetric ($l = 0$) modes with $n_i = 10^{13}\,\mathrm{cm}^{-3}$, and $n_b = 10^{12}\,\mathrm{cm}^{-3}$. $\beta_0 = 0.99$ in 0. 4 and Fig. 5 is drawn for different values of β_0.

https://doi.org/10.1017/S0022377810000632 Published online by Cambridge University Press

Multiplying (18) by r and taking the limit $r \to 0$, with finite $\tilde{n}$ on the axis, yields

$$\left.\frac{\mathrm{d}\tilde{\varphi}}{\mathrm{d}r}\right|_{r=0} = C\left.\frac{l\tilde{\varphi}}{r}\right|_{r=0,} \tag{24}$$

where C is a nonzero and finite constant. Equation (24) yields the conditions on $\tilde{\varphi}$ and its derivatives for the points on the axis. For symmetric modes with $l = 0$, $\tilde{\varphi}_{(r=0)}$ is arbitrary, and we have $(\mathrm{d}\tilde{\varphi}/\mathrm{d}r)|_{r=0} = 0$, which is used in the numerical solution leading to Fig. 4. It is evident from Fig. 4 that the amplitude of the wave depends on the value of $\tilde{\varphi}$ on the axis, which is arbitrarily taken as 1. Therefore, different amplitudes will be obtained for different values of $\tilde{\varphi}$ on the axis.

Figure 4 also shows that for $\beta_0 = 0$ (shown by circles) the electric field for SC_{01} mode, which is represented by the slope of $\tilde{\varphi}$, is zero at $r = 0$, increases gradually, and is distributed almost evenly through out the beam cross section. In the relativistic case, the electric field of SC_{01} mode is concentrated at $0.03 < r/r_b < 0.2$ and is strongest at $0.03 < r/r_b < 0.1$. It should be noted that there is no singularity and the energy density of the electric field represented by the square of the electric field, which is large at some points, remains finite every where. This shows that the relativistic effects concentrate the electric field energy of the symmetric space-charge mode SC_{01} into a thin cylindrical shell, which becomes thinner and moves toward the axis as the energy of the beam is increased. Similar behavior for SC_{02} and SC_{03} are expected.

Figure 5 shows the potential distribution of SC_{01} mode for different beam velocities β_0. This shows that potential drop from axis to the beam edge is gradual for nonrelativistic velocities but becomes sharper and concentrated near the axis as the beam reaches relativistic velocities. For the asymmetric modes with $l \neq 0$, the right-hand side of (24) implies $\tilde{\varphi}_{(r=0)} = 0$ and $(\tilde{\varphi}/r)|_{r=0}$ becomes indeterminate and can have any finite value. These properties of (24) indicate an arbitrary value for $(\mathrm{d}\tilde{\varphi}/\mathrm{d}r)|_{r=0}$. Therefore, for $l = 1$ modes $\tilde{\varphi} = 0$ and $\mathrm{d}\tilde{\varphi}/\mathrm{d}r$ is arbitrary for the points near the axis. Our numerical scheme revealed these two properties. Therefore, for $l = 1$ modes, (18) is solved with $\tilde{\varphi} = 0$ at $r = 0$ and $r = r_b$ and $(\mathrm{d}\tilde{\varphi}/\mathrm{d}r)|_{r=0}$ is set arbitrarily, leading to Fig. 6.

The electrostatic potential of the space-charge mode SC_{11} for the zero axial velocity $\beta_0 = 0$ is compared numerically and analytically using (22). Again, complete agreement between the numerical and analytical results is found. The slope $(\mathrm{d}\tilde{\varphi}/\mathrm{d}r)|_{r=0}$ for the numerical solution is taken equal to that of the analytical solution, which means equal amplitudes for both solutions.

4. Conclusion

Differential equations for the electrostatic waves in relativistic charged particle beams with rotating equilibrium do not have analytical solution, in general, and can only be solved rather with simplifying assumptions or at asymptotic limits [12]. In order to study these modes under more general conditions, numerical methods should be used.

In this analysis, a numerical method is developed to solve the eigenvalue problem of space-charge waves in a relativistic electron beam with ion-channel guiding that completely fills a cylindrical and metallic waveguide. Equilibrium consists of uniform and rigid rotation of the beam without betatron oscillation. The numerical

https://doi.org/10.1017/S0022377810000632 Published online by Cambridge University Press

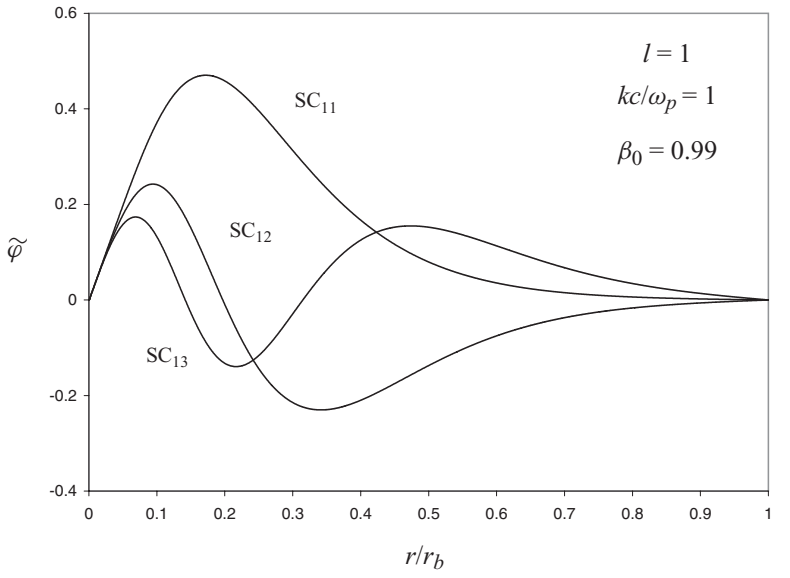


Figure 6. Electrostatic potential $\tilde{\varphi}$ as a function of the normalized radial distance r/r_b for nonsymmetric ($l = 1$) modes, for $n_i = 10^{13}\,\mathrm{cm}^{-3}$, $n_b = 10^{12}\,\mathrm{cm}^{-3}$, $kc/\omega_p = 1$, and $\beta_0 = 0.99$.

technique consists of the finite difference scheme using a shooting method. The eigenvalue problem is a second-order linear differential equation for the electrostatic potential with appropriate boundary conditions. The aim is to find the eigenvalue ω and the eigenfunction $\tilde{\varphi}$ to study dispersion characteristics and find structures of the symmetric and nonsymmetric modes of the space-charge waves. Numerical results were compared with analytical solutions at asymptotic limit of zero axial velocity, and very good agreement was found.

It was found that nonsymmetric ($l = 1$) modes have much higher frequency than the symmetric ($l = 0$) modes, and their frequency approaches the asymptotic value faster as the wave number is increased. For the symmetric ($l = 0$) modes, $\tilde{E}_\theta = \partial\tilde{\varphi}/\partial\theta = 0$, and the transverse component of the electric field is in the radial direction. It was found that at the center of the beam the electric field has no transverse component. For nonsymmetric ($l = 1$) modes, space-charge waves have longitudinal and transverse components everywhere inside the beam.

The distribution of the electric field energy in the radial profile has also been studied. In the nonrelativistic limit, the electric field is distributed comparatively uniformly over the beam cross section. Relativistic motion of the beam in the axial direction pushes the electric field energy toward the axis and concentrates it into a thin cylindrical shell, which becomes thinner and moves toward the axis as the energy of the beam is increased. This effect is more profound for the SC_{01} modes, which is the main harmonic compared to the other modes. Therefore, by using ultrarelativistic beams, it is possible to obtain large electric field energy densities at the center of the beam. This can have important applications in free-electron devices, where space-charge waves are involved in the generation of electromagnetic radiation. Therefore, we have shown that dispersion characteristics and electric field

https://doi.org/10.1017/S0022377810000632 Published online by Cambridge University Press

structures of space-charge waves of a relativistic electron beam are considerably different than that of a nonrelativistic beam with ion-channel guiding.

For $l = 0$ modes, the boundary conditions $\tilde{\varphi}(r = 0) =$ finite and $\tilde{\varphi}(r = r_b) = 0$ also specify the amplitude. For $l = 1$ modes, the boundary conditions are $\tilde{\varphi}(r = 0) = 0$ and $\tilde{\varphi}(r = r_b) = 0$, and the amplitude is specified by the arbitrary slope $(\mathrm{d}\tilde{\varphi}/\mathrm{d}r)|_{r=0}$. The modes with $l \geqslant 2$, which were not studied herein, have boundary conditions similar to the $l = 1$ modes. Comparison of the results of the present investigation with that of the relativistic electron beam with axial magnetic field can also be an interesting problem.

References

[1] Lacambe, C., Mangeney, A., Harvey, C. C. and Scudder, J. D. 1985 *J. Geophys. Res.* **90**, 73.

[2] Lin, R. P., Levedahl, W. K., Letko, W., Gurnett, D. A. and Scarf, F. L. 1986 *Astrophys. J.* **308**, 954.

[3] Celata, C. M. 2000 In: *Proc. XXth Int. Linac Conf., Monterey, CA* (ed. A. W. Chao) (SLAC Report No. SLAC-R-561), p. 668.

[4] Freund, H. P. and Antonsen, T. M., Jr. 1992 *Principles of Free-electron Lasers*. London: Chapman and Hall.

[5] Marshall, T. C. 1985 *Free-Electron Laser*. New York: Macmillan Publishing Co..

[6] Davidson, R. C. 1990 *An Introduction to the Physics of Nonneutral Plasmas*. Redwood City, CA: Addison-Wesley, p. 289.

[7] Spencer, R. L. and Rasband, S. N. 1997 *Phys. Plasmas* **4**, 53.

[8] Davidson, R. C. and Felice, G. M. 1998 *Phys. Plasmas* **5**, 3497.

[9] Goswani, P., Bhattacharyya, S. N., Sen, A. and Maheshwari, K. P. *Phys. Plasmas* **6**, 3442.

[10] Bhattacharyya, S. N. *Phys. Plasmas* **7**, 4805.

[11] Kervalishvili, G. N., Javakhishvili, J. I. and Kervalishvili, N. A. 2002 *Phys. Lett*. A **296**, 289.

[12] Davidson, R. C. 1990 *An Introduction to the Physics of Nonneutral Plasmas*. Redwood City, CA: Addison-Wesley, p. 240.

[13] Dubin, D. H. E. 1991 *Phys. Rev. Lett*. **66**, 2076.

[14] Gould, R. W. 1995 *Phys. Plasmas* **2**, 1404.

[15] Book, D. L. 1995 *Phys. Plasmas* **2**, 1398.

[16] Bhattacharyya, S. N. and Bhattacharjee, A. *Phys. Plasmas* **4**, 895.

[17] Goswani, P., Bhattacharyya, S. N. and Sen, A. 2000 *J. Comput. Phys*. **159**, 312.

[18] Spencer, R. L. 1995 Numerical modeling of nonneutral plasmas. In: *Nonneutral plasma Physics II*. New York: American Institute of Physics, p. 204.

[19] Gammel, G., Nation, J. A. and Read, M. E. 1979 *J. Appl. Phys*. **50**, 5603.

[20] Zou, Y., Wang, J. G., Suk, H. and Reiser, M. 2000 *Phys. Rev. Lett*. **84**, 5138.

[21] Wang, J. G., Wang, D. X. and Reiser, M. 1993 *Phys. Rev. Lett*. **71**, 1836.

[22] Wang, J. G. and Reiser, M. 1998 *Phys. Plasmas* **5**, 2064.

[23] Tian, K., Zou, Y., Cui, Y., Haber, I., Kishek, R. A., Reiser, M. and O'Shea, P. G. 2006 *Phys. Rev. ST Accel. Beams* **9**, 014201.

[24] Gelani, G., Saldin, E., Schneidmiller, E. and Yurkov, M. 2005 *Nucl. Instrum. Methods Phys. Res.* A **554**, 20.

[25] Pinhasi Y. and Gover, A. 1993 *Phys. Rev.* E**48**, 3925.

[26] Wang, J. G., Wang, D. X., Suk, H. and Reiser, M. 1995 *Phys. Rev. Lett*. **74**, 3153.

[27] Chain, A. C. L. 1989 *Phys. Rev.* A **39**, 2561.

https://doi.org/10.1017/S0022377810000632 Published online by Cambridge University Press

[28] Ueda, T. and Shiazawa, T. 1996 *Appl. Phys. Lett*. **69**, 2935.
[29] Cairns, I. H. 1989 *Phys. Fluids* B **1**, 204.
[30] Briggs, R. J. 1976 *Phys. Fluids* **19**, 1257.
[31] Geloni, G., Saldin, E. L., Schneidmiller, E. A. and Yurkov, M. V. 2004 In: *Proc. 26th Int. Free Electron Laser Conference*, Trieste (ed. R. Bakker et al.). Italy: Comitato canferenze Elettra, p. 22.
[32] Saldin, E. L., Schneidmiller, E. A. and Yurkov, M. V. 2002 *Nucl. Instrum. Methods Phys. Res.* A **486**, 516.
[33] Reiche, S. and Rosenzweig, J. B. 2003 *Phys. Rev. ST Accel. Beams* **6**, 040702.
[34] Huang, Z., Borland, M., Emma, P., Wu, J., Limborg, C., Stupakov, G. and Welch, J. 2004 *Phys. Rev. ST Accel. Beams* **7**, 074401.
[35] Martin, W. E., Caporaso, G. J., Fawley, W. M., Prosnitz, D. and Cole, A. G. 1985 *Phys. Rev. Lett*. **54**, 685.
[36] Caporaso, G. J., Rainer, F., Martin, W. E., Prono, D. S. and Cole, A. G. 1986 *Phys. Rev. Lett*. **57**, 1591.
[37] Takayama, K. and Hiramatsu, S. 1998 *Phys. Rev*. A **37**, 173.
[38] Ozaki, T., Ebihara, K., Hiramatsu, S., Kimura, Y., Kishuro, J., Monaka, T., Takayama, K. and Whittum, D. H. 1992 *Nucl. Instrum. Methods Phys. Res.* A **318**, 101.
[39] Yu, L. H., Sessler, A. M. and Whittum, D. H. 1992 *Nucl. Instrum. Methods Phys. Res.* A **318**, 721.
[40] Rouhani, M. H. and Maraghechi, B. 2006 *Phys. Plasmas* **13**, 083101.
[41] Tang, C. J., Liu, P. K. and Liu, S. G. 1996 *J. Phys.* D: *Appl. Phys.* **29**, 90.
[42] Stenflo, L. 1976 *J. Plasma Phys.* **21**, 333.

https://doi.org/10.1017/S0022377810000632 Published online by Cambridge University Press